Acta Biomaterialia 6 (2010) 160–169

Contents lists available at ScienceDirect

Acta Biomaterialia

journal homepage: www.elsevier.com/locate/actabiomat

Post microtextures accelerate cell proliferation and osteogenesis

Eun Jung Kim [a,b], Cynthia A. Boehm [a,c], Alvaro Mata [d], Aaron J. Fleischman [a], George F. Muschler [a,c], Shuvo Roy [a,e,*]

[a] BioMEMS Laboratory, Department of Biomedical Engineering, Lerner Research Institute, Cleveland Clinic, 9500 Euclid Avenue, Cleveland, OH 44195, USA
[b] Department of Chemical and Biomedical Engineering, Cleveland State University, 2121 Euclid Avenue, Cleveland, OH 44115, USA
[c] Department of Orthopaedic Surgery and Orthopaedic Research Center, Cleveland Clinic, 9500 Euclid Avenue, Cleveland, OH 44195, USA
[d] Nanotechnology Platform, Parc Cientific de Barcelona, Baldiri Reixac 10, Barcelona 08028, Spain
[e] Department of Bioengineering and Therapeutic Sciences, University of California – San Francisco, Byers Hall, Room 203A, MC 2520, 1700 4th Street, San Francisco, CA 94158, USA

ARTICLE INFO

Article history:
Received 16 October 2008
Received in revised form 8 May 2009
Accepted 10 June 2009
Available online 16 June 2009

Keywords:
Polydimethylsiloxane
Microfabrication
Soft lithography
Connective tissue progenitor cells
Adult stem cells

ABSTRACT

The influence of surface microtexture on osteogenesis was investigated in vitro by examining the proliferation and differentiation characteristics of a class of adult stem cells and their progeny, collectively known as connective tissue progenitor cells (CTPs). Human bone marrow-derived CTPs were cultured for up to 60 days on smooth polydimethylsiloxane (PDMS) surfaces and on PDMS with post microtextures that were 10 μm in diameter and 6 μm in height, with 10 μm separation. DNA quantification revealed that the numbers of CTPs initially attached to both substrates were similar. However, cells on microtextured PDMS transitioned from lag phase after 4 days of culture, in contrast to 6 days for cells on smooth surfaces. By day 9 cells on the smooth surfaces exhibited arbitrary flattened shapes and migrated without any preferred orientation. In contrast, cells on the microtextured PDMS grew along the array of posts in an orthogonal manner. By days 30 and 60 cells grew and covered all surfaces with extracellular matrix. Western blot analysis revealed that the expression of integrin α5 was greater on the microtextured PDMS compared with smooth surfaces. Real time reverse transcription-polymerase chain reaction revealed that gene expression of alkaline phosphatase had decreased by days 30 and 60, compared with that on day 9, for both substrates. Gene expression of collagen I and osteocalcin was consistently greater on post microtextures relative to smooth surfaces at all time points.

1. Introduction

The response of cells to a substrate surface is strongly influenced by its properties, such as chemical composition and physical topography. These surface characteristics have important implications in the rational design and optimization of biological implants and bioreactors [1–5]. Recent advances in microelectromechanical systems (MEMS) technology provide new opportunities for the investigation of a variety of biological phenomena [6]. For example, soft lithography has been used to pattern the distribution of various chemistries on a material surface to explore selective cellular responses to specific biomolecular species [5]. Microfabrication and related MEMS techniques also enable precise production of surface topographical features to investigate the effects of physical cues on cellular behavior [4–7]. For tissue engineering applications these techniques could be conceptually combined with conventional scaffold processing strategies to ultimately provide scaffolds that possess precise topographical, spatial and chemical properties to optimize control over cellular behavior.

Numerous studies have been conducted to show that different surface topographies influence bone cell behavior [2–10]. For example, Hamilton et al. [7] reported increased cell proliferation and enhanced osteoblast differentiation on discontinuous edge surfaces compared with smooth ones and Mata et al. [8] reported an apparent increase in the proliferation of the progeny of bone marrow-derived connective tissue progenitors (CTPs) on polydimethylsiloxane (PDMS) micro-posts compared with identical cells cultured on smooth PDMS surfaces. CTPs are a heterogeneous population of stem and progenitor cells that are resident in native tissue. These cells are capable of proliferating and giving rise to progeny which contribute directly to the formation of one or more connective tissues [11]. Harvest and transplantation, and even concentration, of CTPs from native bone marrow have been known to improve bone graft efficiency [12,13]. A characteristic of many marrow-derived CTPs is their ability to give rise to progeny that are capable of differentiating along a number of mesenchymal lineages, including bone, cartilage, muscle and fat [11–13].

Osteoblastic differentiation is particularly relevant to clinical bone repair strategies. Fig. 1 illustrates a generally accepted

* Corresponding author. Address: Department of Bioengineering and Therapeutic Sciences, University of California – San Francisco, Byers Hall, Room 203A, MC 2520, 1700 4th Street, San Francisco, CA 94158, USA. Tel.: +1 415 514 9666; fax: +1 415 514 9766.
E-mail address: shuvo.roy@ucsf.edu (S. Roy).

1742-7061
doi:10.1016/j.actbio.2009.06.016

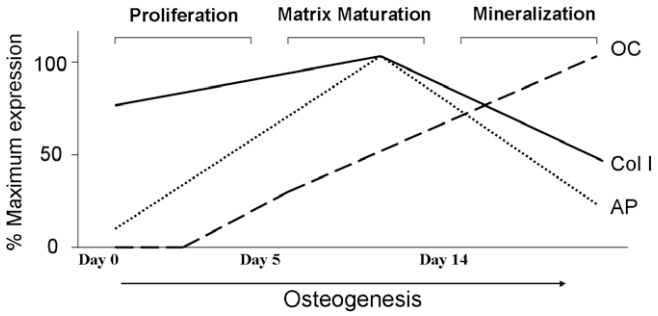

Fig. 1. Qualitative illustration of the three major periods of cell and tissue development in bone formation [14,15]. Relationship between cell growth and differentiation-related gene expression during the in vitro cultivation of osteoblast progenitor cells. Three stages of maturation are reflected by maximal expression of growth and differentiation markers. At the early stage, osteoblast progenitor cells synthesize significant levels of Col I to support matrix formation. Although Col I levels are highest during the proliferation stage, matrix deposition continues to increase throughout the entire culture period. The termination of growth and accumulated extracellular matrix (ECM) accelerates upregulation of AP, an early stage marker of osteogenesis. OC is expressed towards the end of the proliferation stage, during development of the osteoblast phenotype, and reaches peak levels during mineralization. The timescales are derived from data from human mesenchymal stem cells (MSCs) which were culture expanded. In contrast, connective tissue progenitor (CTP) cells are primary bone marrow-derived cells and the corresponding timescale for osteogensis is not known. AP, alkaline phosphatase; Col I, collagen type I; OC, osteocalcin.

pattern of gene expression that reflects three major periods of cell and tissue development in bone formation [14,15]. The differentiated osteoblast is typically characterized by a specific pattern of gene expression, such as alkaline phosphatase (AP), collagen and osteocalcin (OC), and in vitro mineralization capacity [1,14,15].

In our previous study [8], human bone marrow-derived CTPs were cultured for 9 days on smooth PDMS surfaces and on PDMS with post microtextures that were 6 μm high and either 5, 10, 20 or 40 μm in diameter. We discovered that cells on microtextured PDMS exhibited a different morphology and increased cell count relative to those on a smooth PDMS surface. In particular, our investigations showed that 10 μm diameter post textures significantly enhanced CTP growth. This result suggested that, despite identical surface chemistries, the substrate topography had a significant effect on the biological performance of CTPs and suggested a potential role for microtextured materials in bone tissue engineering applications. In the current study, we investigate the influence of microtextured surfaces on proliferation and osteogenic differentiation of CTP progeny in long-term culture. Human marrow-derived CTPs were plated in primary culture on PDMS substrates presenting either post microtextures or a control (smooth) surface for up to 60 days, as an in vitro model to investigate the potential response of CTPs to different surface textures in a bone healing environment in vivo.

2. Materials and methods

2.1. Substrate preparation

The microfabricated PDMS substrate was produced by soft lithography techniques [8]. Briefly, a 6 μm thick layer of SU-8 2010 negative photoresist was first coated on top of a silicon (Si) wafer. Using an ultraviolet (UV) photolithography process, the 10 μm diameter and 6 μm high micro-post pattern, with 10 μm separation between posts, was then transferred from a photomask to the photoresist. Afterwards, this SU-8 mold was coated with 1H,1H,2H,2H-perfluorodecyltrichlorosilane (Lancaster Synthesis, Pelham, NH) to aid the release of PDMS in the final step of substrate production. The liquid PDMS base and curing agent (Sylgard 184, Dow Corning, Midland, MI) components were subsequently mixed at a ratio of 10:1, degassed for 20 min and then poured uniformly on top of the patterned SU-8 mold. After additional degassing for 10 min, the PDMS was cured at 85 °C for 2 h or at room temperature for 1 day (Fig. 2a). The cured PDMS cast was finally released from the mold and sectioned into 2×2 cm samples. Representative samples were inspected by scanning electron microscopy (SEM) (JSM-5310, JEOL USA, Peabody, MA). An unpatterned SU-8 mold was used to produce the smooth PDMS surface, which served as the control substrate for our study (Fig. 2b).

2.2. Cell culture

As described by Muschler et al. [16], bone marrow aspirates were harvested from the anterior iliac crest with informed consent from three patients immediately prior to elective orthopedic procedures. Briefly, a 2 ml sample of bone marrow was aspirated from the anterior iliac crest into 1 ml saline containing 1000 U heparin (Vector Labs, Burlingame, CA). The heparinized marrow sample was suspended in 20 ml heparinized carrier media (α-minimal essential medium (MEM) + 2 U ml^{-1} of Na-heparin) (Gibco, Grand Island, NY) and centrifuged at 1500 rpm (400*g*) for 10 min. The buffy coat was collected, resuspended in 20 ml 0.3% bovine serum albumin–MEM (Gibco) and the number of nucleated cells was counted. The PDMS substrates were sterilized for 30 min with 70% ethanol and placed inside standard tissue culture dishes (Chamber Slide System, Lab-Tek, Naperville, IL). Cells were then plated on day 0 at a seeding concentration of 1×10^6 cells per well (2×2 cm) and cultured for up to 60 days under conditions promoting osteoblastic differentiation [16].

In previous studies [11,16] we established that CTPs exhibit an osteoblastic phenotype after 9 days of culture. In order to determine possible effects of surface topography on the transition of cells from the lag to the log phase, cell counts were performed daily for the first 10 days and subsequently on days 30 and 60.

2.3. Cell morphology

On days 9, 30 and 60 the medium was removed and the plated substrates were placed in a solution containing 2% glutaraldehyde (Electron Microscopy Sciences, Fort Washington, PA), 3% sucrose (Sigma–Aldrich Co., Irvine, UK) and 0.1 M phosphate-buffered saline (PBS) (Cambrex BioScience, Wlkersville, MD) at 4 °C and pH 7.4. After 1 h the substrates were rinsed twice with PBS for 30 min at 4 °C and washed with distilled water for 5 min. Dehydration was achieved by placing the plated substrates in 50% ethanol for 15 min while increasing the concentration of ethanol sequentially to 60%, 70%, 80%, 90% and finally 100%. Dehydrated samples were then critical point dried, mounted on aluminum stubs, sputter-coated with gold–palladium and examined using SEM (JSM-5310, JEOL USA).

2.4. Cell proliferation and differentiation

2.4.1. PicoGreen DNA quantification

CTP progeny seeded substrates were resuspended with 50 μl lysis buffer (1% sodium dodecyl sulfate, 10 mM ethylenediaminetetraacetic acid (EDTA) and 50 mM Tris–HCl, pH 8.1) (Sigma–Aldrich Co.) to lyse the membranes of adherent CTP progeny. After 60 min the samples were centrifuged at 14,000 rpm for 5 min and the supernatant was removed for analysis. A 40 μl sample of aqueous supernatant containing DNA was added to 0.96 ml TE buffer (10 mM Tris adjusted to pH 7.0 with HCl,

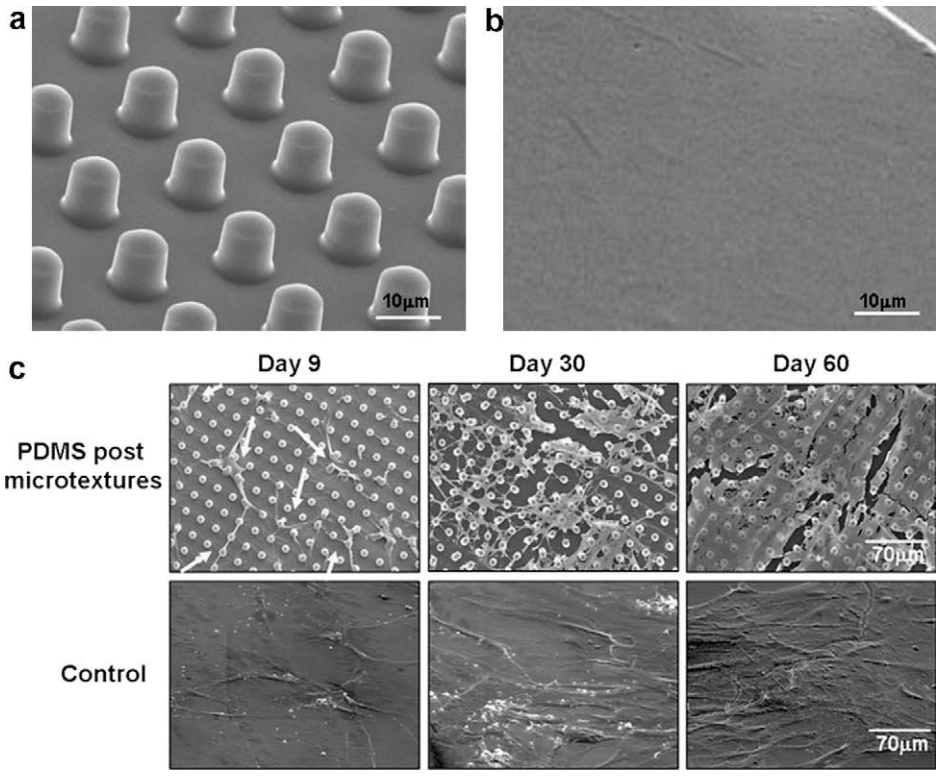

Fig. 2. SEM images of PDMS substrates and CTPs on PDMS post microtextures and control surfaces on days 9, 30 and 60. The PDMS substrates were produced by soft lithography techniques. (a) PDMS post microtextures 6 μm in height and 10 μm in diameter, with 10 μm separation between posts. (b) Control (smooth PDMS) surface. (c) CTPs attached to post microtextures and control surfaces with varying cell morphologies. On post microtextures on day 9 CTPs mostly tended to attach next to the posts and spread between them while directing their processes towards posts and other cells. On day 30 we can see increased cell growth on the post microtexture scaffolds. By day 60 numerous cells had grown and spread over the top of the post microtextures and covered most of surface with ECM. In contrast, cells on the control surfaces exhibited arbitrary flattened shapes and migrated without any preferred orientation for up to 60 days.

1 mM EDTA) (Molecular Probes, Eugene, OR). As per the manufacturer's instructions (Molecular Probes), stock PicoGreen reagent was diluted 1:200 in TE buffer and 1 ml of that was added to each DNA-containing sample. The tubes were capped, vortexed and incubated at room temperature in a dark room for 3 min. The fluorescence was measured with a SpectraMax Gemini fluorescence microplate reader (Molecular Devices Co., Sunnyvale, CA), with excitation and emission wavelengths of 480 and 520 nm, respectively. All calibration samples were assayed four times and a fresh calibration curve was generated for each 96-well plate. Baseline fluorescence was determined with a TE blank, the average of which was subtracted from the averaged fluorescence of other samples. Using this analysis, we determined a DNA concentration of $\sim$4.5 μg in 1×10^6 adherent CTPs. Thus, we estimated total cell number by assuming that 4.5 pg of DNA represents one cell. Also, we performed a calculation to determine that, for identical projected surface areas, the actual surface area of post microtextures was 1.47 times greater than that of the smooth (control) surface. Consequently, we divided the total cell number (estimated via DNA quantification) from the post microtextures by 1.47 to enable a meaningful comparison with the cell number from smooth surfaces.

2.4.2. DAPI stain

Cell nuclei were stained with 6-diamidino-2-phenylindole dihydrochloride hydrate (DAPI). Ethanol-fixed cells were rinsed three times with PBS and then a 10 μl drop of DAPI-containing Vectashield mounting medium (Vector Labs) was placed on the substrates. Immediately thereafter the edges of the coverslips were sealed with three coats of clear nail polish and viewed under a fluorescence microscope (BX50F, Olympus Optical Co., Japan).

2.4.3. Alkaline phosphatase (AP) stain

Cells were stained for AP using Vector Red substrate working solution (5 ml 100 mM Tris–HCl with the addition of 2 drops of reagents 1, 2 and 3) (Vector Labs) for 30 min at room temperature in the dark, and then washed in distilled water. The positively stained cells with AP activity appeared red when viewed under a fluorescent microscope.

2.4.4. von Kossa stain

Cells were rinsed with PBS and fixed in 4% paraformaldehyde (Electron Microscopy Sciences) for 1 h. They were then incubated in 5% silver nitrate (Sigma–Aldrich Co.) for 30 min in a dark room, rinsed with distilled water and exposed to UV light for 1 h. Secretion of calcified extracellular matrix (ECM) was confirmed as deep blue-purple nodules with von Kossa staining under a phase contrast microscope.

2.5. Integrin expression

Integrin expression was confirmed by Western blot analysis. Cell extracts were prepared by adding lysis buffer containing 10 mM Tris–HCl, 5 mM EDTA, 150 mM NaCl, 30 mM sodium pyrophosphate, 50 mM NaF, 10% glycerol and a cocktail of protease inhibitors (Sigma–Aldrich Co.). Lysates were clarified by centrifugation at 13,000 rpm for 15 min at 4 °C and the protein content of supernatants was determined using a modified Bradford assay (Bio-Rad, Hercules, CA). Diluted 15 μg protein samples were loaded onto a 10% Tris–HCl ready gel (Bio-Rad) and electrophoresed in SDS running buffer at 130 V for 2 h. The proteins were electrophoretically transferred onto a Hybond-P membrane (Amersham Pharmacia Biotech, Piscataway, NJ) in 1× transfer buffer at 100 V for 2 h in a cold room (4 °C).

Membranes were blocked with 5% skimmed milk and PBS containing 0.1% Tween (TPBS) at room temperature for 1 h. Primary antibodies (integrins α1, α2, α5 and β1 and GAPDH) (Chemicon, Temecula, CA) were diluted 1/200–1/1000 in 5% skimmed milk and incubated with the membranes overnight. After washing the membranes three times in TPBS they were incubated for 1 h with 1/1000 horseradish peroxidase (HRP)-conjugated secondary antibody (Chemicon). The membrane was washed again three times in TPBS and the signals were visualized using ECL detection reagents (Amersham Pharmacia) for 3 min and exposed to radiographic film (Eastman Kodak, Rochester, NY) for 30 s to 10 min. The intensity of the exposed bands was measured using the Gel-Pro program (Gel-Pro Analyzer version 3.1., Silver Spring, MD) to quantify protein expression.

2.6. Gene expression

2.6.1. Real time reverse transcription-polymerase chain reaction (real time RT-PCR)

Expression of osteoblast-specific genes, such as AP, type I collagen (Col I) and OC, were detected by real time RT-PCR. Total cellular RNA was isolated using a RNeasy kit (Qiagen Inc., Valencia, CA) and reverse transcribed by conventional protocols with a Sensiscript Reverse Transcription kit (Qiagen Inc.). Expression of AP, Col I, OC and glyceraldehyde-3-phosphate dehydrogenase (GAPDH) was quantified using real time RT-PCR analysis with a Power SYBR® Green PCR Master Mix kit (Applied Biosystems, Foster City, CA). GAPDH is an enzyme utilized in cellular metabolism and is assumed to be expressed at the same level in most cells, therefore gene expression of GAPDH was used as an internal control to normalize for any differences in amount of total RNA isolated [16]. Real time quantitative PCR was performed on a 7500 Real Time PCR system (Applied Biosystems). Data analysis was carried out using 7500 System Sequence Detection software (Applied Biosystems) [17].

2.7. Statistical analysis

The PicoGreen DNA quantification and real time RT-PCR analyses were each performed a total of nine times (three replicates for each of the three patients, i.e. $n = 9$ for each substrate) as per our standard laboratory protocols. The mean and standard deviation (SD) values were subsequently calculated using the data of all groups. Statistical analysis ($n = 9$) was performed by a one-way analysis of variance (ANOVA) with Tukey's multiple comparison test (SPSS Version 10.0., SPSS Inc., Chicago, IL) with a significance level of $P < 0.05$ (the 95% confidence interval).

3. Results

3.1. Cell morphology

The SEM images revealed that human CTPs attached to PDMS substrate surfaces showed varying cell morphologies (Fig. 2c). CTP progeny on the smooth surfaces exhibited arbitrary flattened shapes and migrated without any preferred orientation for up to 60 days. In contrast, on day 9 CTP progeny on PDMS post microtextures mostly tended to attach next to the posts and spread between them while directing their processes towards other posts and cells. On day 30 increased cell growth was observed on the post microtexture substrates. By day 60 numerous cells had grown and spread over the top of the post microtextures and covered most of the surface with ECM.

3.2. Early cell growth

CTP cultures from all three donors expanded with characteristic lag and log phases (Fig. 3a). DNA quantification analysis revealed that the number of cells initially attached (day 1) to the PDMS substrates were almost identical (391 cells cm^{-2} for smooth and 361 cells cm^{-2} for microtextured). Furthermore, there were minimal changes in daily cell numbers for both substrates through day 4. On day 5 CTPs on PDMS post microtextures transitioned to log phase, as demonstrated by a 3.6-fold increase in cell number. In contrast, the lag phase of CTPs on smooth surfaces lasted longer, with a 2.1-fold increase in cell number occurring on day 7 (Fig. 3b). After exiting from lag phase the rate of increase in cell number in log phase was similar for both PDMS post microtextures and smooth surfaces.

3.3. Cell proliferation

The CTPs on substrates were viewed in situ on days 9, 30 and 60 by DAPI staining (Fig. 4). The stain revealed that there were qualitatively more cells on PDMS post microtextures than smooth surfaces throughout the culture period. This observation was confirmed by the DNA quantification analysis (Fig. 4). On day 9 PDMS post microtextures supported more than twice the number of cells supported on smooth surfaces. Furthermore, on day 30 the PDMS post microtextures supported over three times the number of cells supported on control surfaces ($P < 0.05$). Finally, on day 60 PDMS post microtextures continued to support almost twice the number of cells compared with control surfaces.

3.4. Integrin expression

The expression of all integrins on day 9 was low, most probably due to the relatively low number of cells (data not shown). On days 30 and 60 Western blot analysis revealed that integrins α1, α2, α5 and β1 were expressed by the cells on all surfaces, although integrin α1 was expressed at generally lower levels (Fig. 5). On day 30 integrins α1, α2 and β1 demonstrated comparable expression levels between post microtextures and smooth surfaces. In contrast, integrin α5 exhibited an almost 3-fold greater expression level on the PDMS post microtextures. On day 60 integrin α5 still exhibited increased expression on PDMS post microtextures compared with smooth surfaces, although the difference had decreased to 1.5-fold.

On day 60 integrins α1, α2 and β1 again demonstrated comparable expression levels between substrates. However, compared with day 30 the actual expression level of α2 had increased over 2-fold, while decreasing very slightly for integrin α1 and increasing slightly for β1. Integrin α5 still exhibited a greater expression level (1.5-fold) on the PDMS post microtextures compared with smooth surfaces. However, compared with day 30 the actual expression on smooth surfaces had increased by almost 2.5-fold, while increasing very slightly for the post microtextures.

3.5. AP expression and mineralization

CTPs on the various PDMS substrates were also viewed in situ on days 9, 30 and 60 using AP and von Kossa staining. In general, cells on the PDMS post microtextures stained more intensely for AP compared with smooth surfaces on day 9 (Fig. 6a). Almost all cells expressed AP on both substrates on days 30 and 60. In contrast, the von Kossa staining was minimal on all substrates on day 9, but increased on day 30, and even further on day 60 (Fig. 6c). The spatial distribution and intensity of the von Kossa stain appeared to be consistently greater on PDMS post microtextures than on the smooth surfaces.

3.6. Gene expression

Expression of key osteoblastic bone markers, such as AP, Col I and OC, was assessed in the CTP progeny on substrates using real

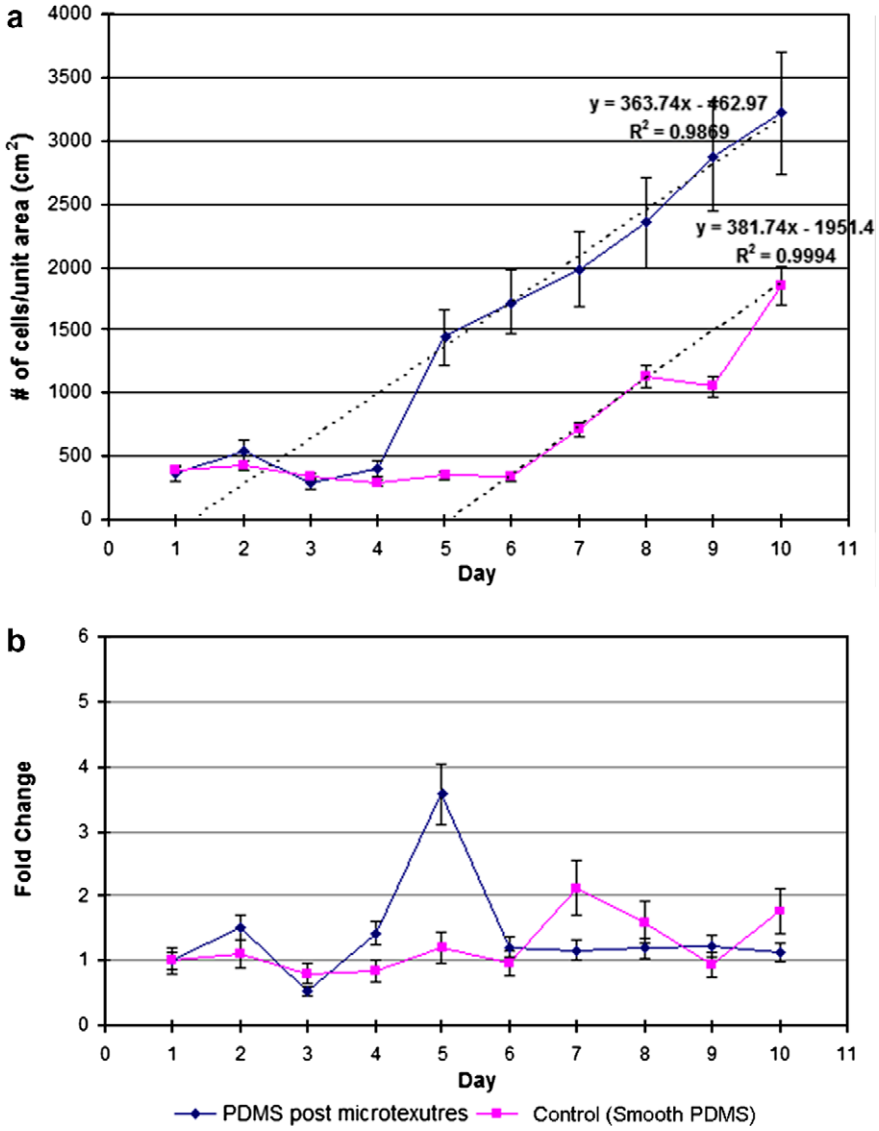

Fig. 3. Time dependent (a) growth curves and (b) fold changes of CTPs attached to PDMS substrates. DNA quantification analysis revealed that the number of CTPs initially attached to PDMS substrates were almost identical. However, the greatest fold change was observed between day 4 and day 5, as the cells on PDMS post microtextures were about to exit from lag phase. Cells on the control surfaces were about to exit from lag phase on days 6 and 7. After exiting from the lag phase, the cell growth curves were similar on PDMS post microtextures and control surfaces.

time RT-PCR. The results revealed that AP expression was higher on PDMS post microtextures on day 9, but decreased on days 30 and 60 (Fig. 6a). Col I expression increased over time on both microtextured and control surfaces, but was consistently greater on microtextured surfaces than on control surfaces (Fig. 6b). Trends in OC expression were similar to Col I, with consistently greater expression on microtextured surfaces, particularly on day 60 (Fig. 6c).

4. Discussion

Understanding and optimizing cell–ECM–substrate surface interactions is critical to the rational design of biological implant materials and tissue engineering scaffolds, particularly for bone healing applications, where the concentration and prevalence of local osteogenic CTPs in native tissues are generally suboptimal [18–22]. We hypothesized that the biological performance of CTPs and their progeny with respect to proliferation, migration and osteoblastic differentiation would be significantly modified by interaction with PDMS post microtextures when compared with control (smooth PDMS) surfaces, as assessed by cell retention, expression of integrins, AP activity, matrix deposition and mineralization associated with osteoblastic differentiation.

Our study shows that the transition of CTP progeny from lag to log phase and associated indicators, such AP expression, collagen and osteocalcin synthesis, mineralization and the expression of integrin $\alpha 5$, were all increased or accelerated on PDMS post microtextures when compared with the smooth surfaces. The choice of PDMS as the construction material for both substrates, and the similarities in processing and handling and identical culture conditions, allow us to gain insights into the role of surface topography on cell growth, since the underlying surface chemistry is identical.

Cellular responses are generally attributed to the surface-adsorbed ECM, which comes from the surrounding medium and can also be produced by cells themselves [20–22]. Cells are known to attach to ECM via integrin receptors, and integrin-mediated attachment affects cell behavior, such as adhesion, migration, proliferation and differentiation [23]. Integrin $\alpha 1\beta 1$ and $\alpha 2\beta 1$ bind to type I collagen, which is the dominant bone matrix protein, and this binding has been reported to regulate osteoblastic differentiation

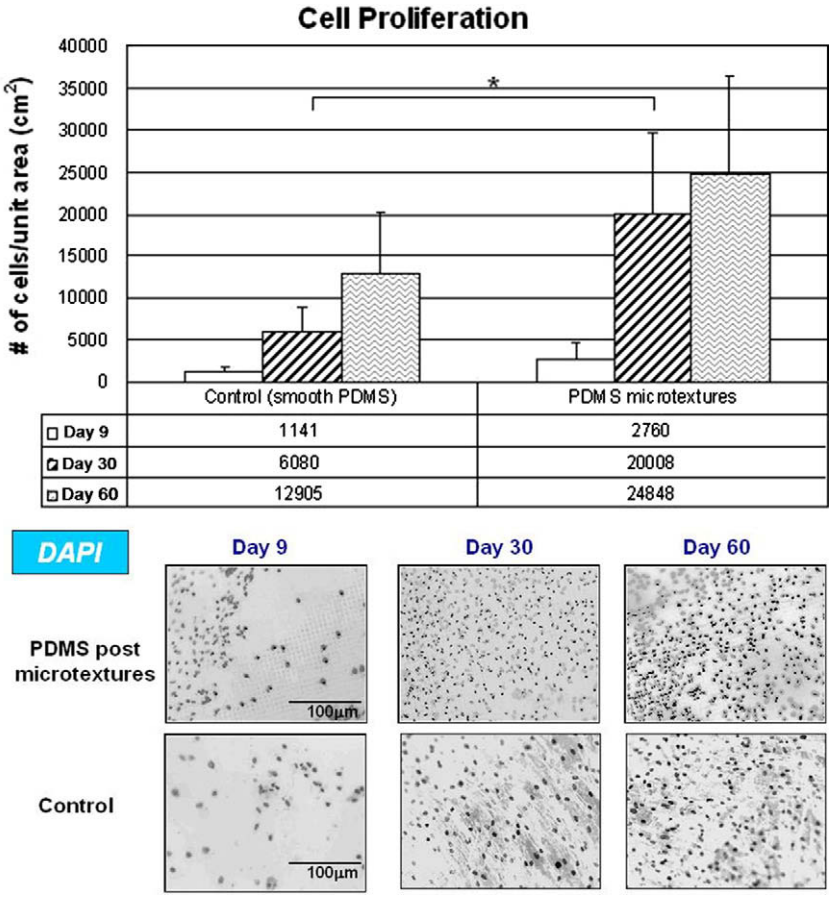

Fig. 4. CTP number on PDMS post microtextures and corresponding control surfaces. On day 9 the number of CTPs on the post microtextures was greater than on the control surfaces. The post microtextures exhibited a significant increase in CTPs on day 30. On day 60 the number of CTPs increased on post microtextures compared with the control surfaces. Fluorescent images show cell nuclei stained with DAPI and reveal more cells on post microtextures than control surfaces. *(Note: the original color images were converted to grayscale and reversed to provide visual clarity).* The PicoGreen DNA quantification was performed a total of nine times (three replicates for each of the three patients, i.e. $n = 9$ for each substrate) as per our standard laboratory protocol. *Statistically significant compared with control surfaces on day 30 ($P < 0.05$).

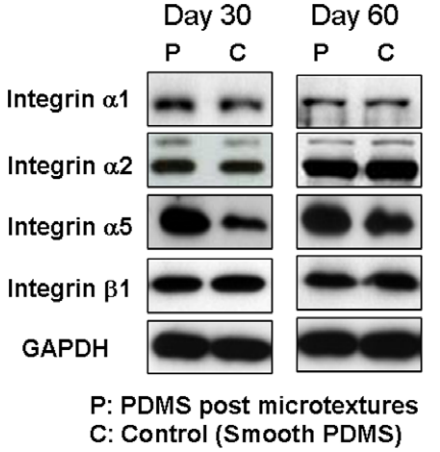

Integrated Optical Density (IOD) values (X 1,000)

	Day 30		Day 60	
	P	C	P	C
α1	20	17.6	16.8	16
α2	32	30.4	70	72
α5	108	32.8	112.5	81
β1	61	65	74	72

Fig. 5. Integrins and GAPDH expression in CTPs after 30 and 60 days culture on PDMS post microtxtures and control surfaces. Integrins α1, α2, α5 and β1 were expressed by the cells on all surfaces, although integrin α1 was expressed at generally lower levels. On days 30 and 60, integrins α1, α2, and β1 showed comparable expression levels between post microtextures and smooth surfaces. In contrast, integrin α5 exhibited greater expression level on the PDMS post microtextures compared with smooth surfaces.

[24]. Binding of integrin α5β1 to ECM is known to regulate osteoblast survival, proliferation, bone-specific gene expression and matrix mineralization [24,25]. In our Western blot results integrin α1 and β1 were expressed similarly over time, while the expression of integrin α5 was greater on the PDMS post microtextures on both days 30 and 60 (Fig. 4). Thus, these data suggest that the increased integrin α5 expression of CTPs on post microtextures resulted in increasing ECM production and subsequent osteoblast-specific gene expression by cells on post microtextures (Fig. 6).

Fig. 4 shows that the cell number on PDMS post microtextures were consistently greater than on the smooth surfaces. The reported cell numbers per unit area have already been adjusted to

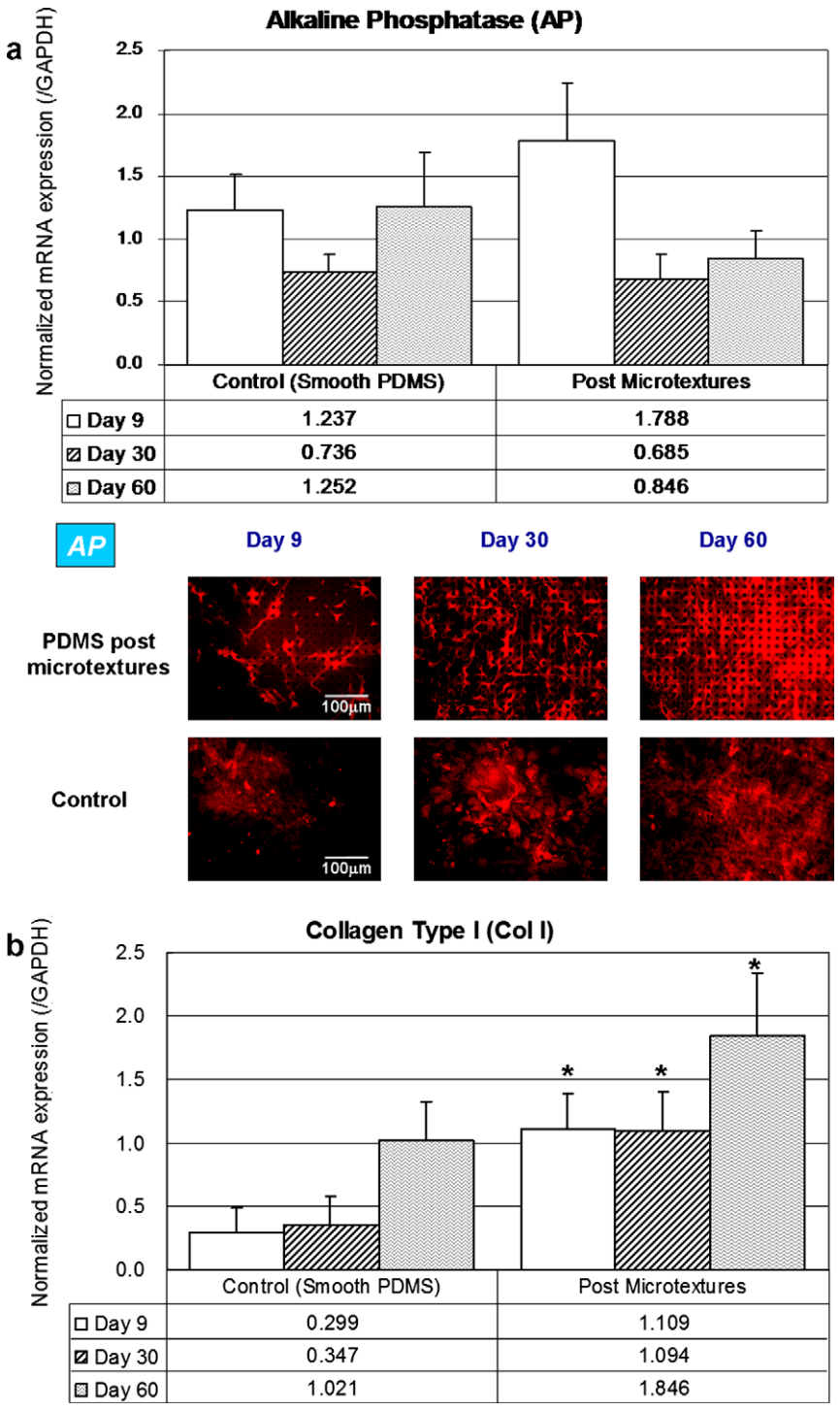

Fig. 6. Gene expression of (a) AP, (b) collagen type I (Col I) and (c) osteocalcin (OC) by CTPs after 9, 30 and 60 day on PDMS post microtextures and control surfaces. (a) AP mRNA expression during development, with the highest levels present on day 9 on post microtextures, while it was expressed more highly on the control surface on day 60. Fluorescent images show cells on the post microtextures stained more intensely for AP compared with control surfaces on day 9, and AP increased on all surfaces by days 30 and 60. (b) mRNA of Col I expression at all time points, with slightly higher expression on day 30 and significantly higher on day 60. (c) Compared with day 9, OC mRNA expression showed a significant increase in cells grown on post microtextures on day 60 compared with cells grown on the control surface. Phase contrast images show von Kossa stain and the intensity of this stain on post microtextures increased with time compared with the control surfaces. The real time RT-PCR was performed a total of nine times (three replicates for each of the three patients, i.e. $n = 9$ per substrate) as per our standard laboratory protocols. *Statistically significant compared with control surfaces on same day ($P < 0.05$).

account for the difference in actual surface areas between post microtextures and smooth surfaces. Furthermore, according to our previous experiments [8] and Fig. 3 the numbers of CTPs attached initially to the PDMS post microtextures and smooth surfaces were almost identical. Therefore, it appears that the enhanced cell growth on post microtextures resulted primarily from the shortened lag phase, which is evident in Fig. 3. The earlier onset of proliferation would lead to increased cell number on days 9, 30 and 60. Presumably, the higher cell number resulted in their early confluence and stimulation of osteogenic differentiation

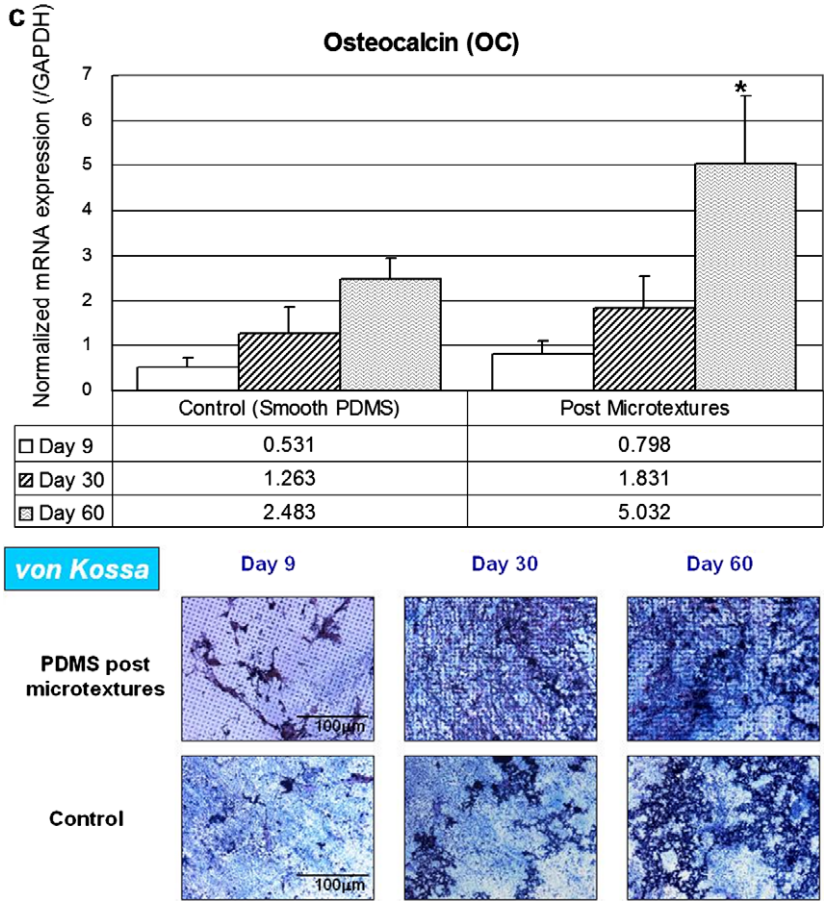

Fig. 6 (*continued*)

(ECM production, osteoblast–ECM related integrin expression and subsequent osteoblast-specific gene expression) on post microtextures.

Larson et al. [26] have investigated the growth of passaged human bone marrow-derived multipotent stromal cells in low density (50 cells cm^{-2}) cultures on standard tissue culture substrates for up to 10 days. In this time frame their cultures expanded with characteristic lag, log and near stationary phases, with the greatest fold change observed on days 2 and 3, when the cells transitioned to log phase. In contrast, our CTPs remained in lag phase for 6 and 4 days for the smooth and microtextured PDMS, respectively. Furthermore, the CTPs continued to proliferate for over 30 days without achieving stationary phase. Possible reasons for the differences in our results from the previous reports could arise from our choice of substrate material (PDMS), culture conditions (high density) and the heterogeneity of the CTP population. Additional investigations will be required to gain further insights into the differences in growth characteristics between CTPs and conventional mesenchymal stem cells.

Numerous groups have examined the effect of surface topographies on cell behavior [27–38]. Table 1 presents a summary of results from previous work and a comparison with the current study. In general, our results are consistent with previous reports which suggest that surface microtopography influences osteogenesis. However, the current study has focused on CTPs, which have not been examined similarly in the past. In addition, we have demonstrated that, in spite of the identical surface chemistry, cells cultured on post microtextures appear to exhibit a shortened lag phase relative to smooth surfaces. Thus, even when the initial numbers of cells attached to the substrates were similar, post microtextures ultimately resulted in increased cell number and appeared to accelerate osteogenesis.

There are many factors contributing to the increased cell numbers and expression of osteogenic markers on different surface topographies. The incorporation of micro- and nano-scale topographies at the cell–substrate interface might provide an attractive approach to enhancing specific cell behavior without destabilizing the delicate biochemical environment. However, the mechanisms by which cell behavior changes in response to different geometrical and biochemical stimuli remain unclear. Further investigation is needed to elucidate all of the possible factors and establish definitive mechanistic links between cell–surface interactions and cell differentiation.

Moreover, demonstrating the feasibility of using CTP surface topography constructs for bone tissue formation will require experiments in an animal model for performance assessment in vivo. These experiments could initially be performed with 3-dimensional scaffolds with different surface topographies to verify enhanced CTP growth characteristics. Afterwards, the performance of 3-dimensional scaffolds should be investigated in an animal model to provide insights into the behavior of these for human bone graft applications.

5. Conclusion

Post microtextures accelerate proliferation and osteogenic differentiation of CTP cultures compared with those on control (smooth) surfaces. This difference in overall cell growth can be attributed to a reduction in lag time between initial cell contact

Table 1
Effect of surface topography on cells.

Reference	Cell type	Time	Surface topography	Investigation/results
[27]	Mg63 osteoblast-like cells	1 Week	Rough Ti surfaces with different morphologies (SLA Ra = 3.3 μm and TPS Ra = 0.22 μm)	Response of MG63 osteoblast-like cells to Ti and Ti alloy is dependent on surface roughness and composition
[28]	Mg63 osteoblast-like cells	1 Week	Ti disks also were sandblasted (SB) and acid etched (CA) or plasma sprayed with Ti particles (PS)	Bone cell response to systemic hormones is modified by surface roughness and surface roughness increases the responsiveness of MG63 cells to 1a,25-(OH)2D3
[29]	Mg63 osteoblast-like cells	5 Days	Rough Ti surfaces with different morphologies (SLA Ra = 3.97 μm and TPS Ra = 5.21 μm)	Both cyclooxygenase-1 and cyclooxygenase-2 mediate osteoblast response to Ti surface roughness
[30]	Human osteoblasts	1 Week	Rough Ti surfaces with different morphologies (SLA Ra = 3.97 μm and TPS Ra = 5.21 μm)	Normal adult human female osteoblasts are sensitive to surface microtopography and E2 can alter this response
[31]	Osteoblasts	3 Weeks	600 Grit (grooved) or sandblasted (roughened) cpTi implant discs	Osteoblast gene expression and mineralization are affected by roughened implant surface microtopographies during osseointegration of dental implants
[32]	Human embryonic palatal mesenchymal cells	3 Weeks	600 Grit (grooved) or sandblasted (roughened) cpTi implant discs	Pre-osteoblast cell differentiation is affected by implant surface microtopographies during osseointegration of dental implants
[33]	Rat osteoblasts	6 Weeks	Discontinuous edge surfaces (DES): 34 × 34–65 × 65 μm in width and 4 and 10 μm in depth	DES alter adhesion, migration and proliferative responses of osteoblasts at early time points and promote multilayering, matrix deposition and mineral deposition at later times
[34]	Mg63 osteoblast-like cells	1 Week	Rough Ti surfaces with different morphologies (SLA Ra = 4 μm and TPS Ra = 0.7 μm)	Physical properties of the submicron scale structures are important variables in determining osteoblast response to substrate topography
[35]	Rat osteoblasts	6 Weeks	(A) 30 μm deep grooves with a 45 μm pitch, (B) 10 μm deep gap cornered boxes and (C), 30 μm deep tapered pits	The effect of substratum topography on osteoblast adhesion mediated signal transduction and phosphorylation
[36]	Epithelial cells and osteoblasts	4 Weeks	TPs and inverted pyramids within the range of 30–120 μm in depth	Tapered pits stimulate osteoblast mineral deposition in vitro and in vivo, but do not prevent epithelial sheet migration
[37]	Human mesenchymal stem cell and osteoprogenitor cells	4 Weeks	PMMA 120 nm diameter pits (100 nm deep, absolute or average 300 nm centre–centre spacing) with displaced square 50 (±50 nm from true centre)	Topographically treated MSCs have a distinct differentiation profile compared with those treated with osteogenic media
[38]	Human mesenchymal stem cell	3 Weeks	PMMA pit (width:deep 30 μm:300 nm or 40 μm:400 nm) and groove (width:deep = 5 μm:500 nm or 50 μm:300 nm)	The nanotopographies allowed control of cell adhesion, cytoskeleton, growth and production of osteoblastic markers
Our data	Human bone marrow-derived CTPs	60 Days	PDMS post microtextures 10 μm diameter and 6 μm height (effective Ra = 3 μm)	PDMS post microtextures accelerate proliferation and osteogenic differentiation of CTPs

with the substrate surface and cell spreading. Cells proliferate in greater numbers, express higher amounts of ECM genes and secrete greater amounts of minerals on the post microtextures than on the control surfaces after long-term culture. The earlier onset of cell proliferation on microtextures results in increased cell numbers, their early confluence and stimulation of osteogenic differentiation. This study demonstrates a valuable in vitro model, based on the precise and reproducible patterning capabilities of microfabrication and related MEMS techniques, in which to explore the relationship between topographical features of bone tissue engineering scaffolds and the likely response of human adult stem cells and progenitor cells in the setting of bone repair in vivo.

Appendix. Figures with essential colour discrimination

Certain figures in this article, particularly Figs. 3, 4 and 6, are difficult to interpret in black and white. The full colour images can be found in the on-line version, at doi: 10.1016/j.actbio. 2009.06.016.

References

[1] El-Amin SF, Botchwey E, Tuli R, Kofron MD, Mesfin A, Sethuraman S, et al. Human osteoblast cells: isolation, characterization, and growth on polymers for musculoskeletal tissue engineering. J Biomed Mater Res 2006;76A:439–49.
[2] Curtis A. Nanofeaturing materials for specific cell responses. Mater Res Soc Symp Proc 2005;845:175–84.
[3] Healy KE, Thomas CH, Rezania A, Kim JE, McKeown PJ, Lom B, et al. Kinetics of bone cell organization and mineralization on materials with patterned surface chemistry. Biomaterials 1996;17:195–208.
[4] Raghavan S, Chen CS. Micropatterned environments in cell biology. Adv Mater 2004;16:1303–13.
[5] Chen CS, Jiang X, Whitesides GM. Microengineering the environment of mammalian cells in culture. MRS Bull 2005;30:194–201.
[6] Roy S, Ferrara LA, Fleischman AJ, Benzel EC. Microelectromechanical systems and neurosurgery: a new era in a new millennium. Neurosurgery 2001;49:779–98.
[7] Hamilton DW, Wong KS, Brunette DM. Microfabricated discontinuous-edge surface topographies influence osteoblast adhesion, migration, cytoskeletal organization, and proliferation and enhance matrix and mineral deposition in vitro. Calcif Tissue Int 2006;78:314–25.
[8] Mata A, Boehm C, Fleischman AJ, Muschler G, Roy S. Growth of connective tissue progenitor cells on microtextured polydimethylsiloxane surface. J Biomed Mater Res 2002;62:499–506.
[9] Tsigkou O, Hench LL, Boccaccini AR, Polak JM, Stevens MM. Enhanced differentiation and mineralization of human fetal osteoblasts on PDLLA containing bioglass composite films in the absence of osteogenic supplements. J Biomed Mater Res A 2007;80(4):837–51.
[10] Anselme K. Osteoblast adhesion on biomaterials. Biomaterials 2000;21:667–81.
[11] Muschler GF, Midura RJ, Nakamoto C. Practical modeling concepts for connective tissue stem cell and progenitor compartment kinetics. J Biomed Biotechnol 2000;3:1–24.
[12] Ratner BD, Bryant SJ. Biomaterials: where we have been and where we are going. Annu Rev Biomed Eng 2004;6:41–75.
[13] Muschler GF, Nakamoto C, Griffith LG. Engineering principles of clinical cell-based tissue engineering. J Bone Joint Surg 2004;86A:1541–58.

[14] Stein GS, Lian JB, van Wijnen AJ, Stein JL, Montecino M, Javed A, et al. Runx2 control of organization, assembly and activity of the regulatory machinery for skeletal gene expression. Oncogene 2004;23:4315–29.
[15] Kulterer B, Friedl G, Jandrositz A, Sanchez-Cabo F, Prokesch A, Paar C, et al. Gene expression profiling of human mesenchymal stem cells derived from bone marrow during expansion and osteoblast differentiation. BMC Genomics 2007;8:70–84.
[16] Muschler GF, Nitto H, Boehm CA, Easley KA. Age- and gender-related changes in the cellularity of human bone marrow and the prevalence of osteoblastic progenitors. J Orthop Res 2001;19:117–25.
[17] Cool SM, Nurcombe V. Substrate induction of osteogenesis from marrow-derived mesenchymal precursors. Stem Cells Dev 2005;14:632–42.
[18] Bruinink A, Wintermantel E. Grooves affect primary bone marrow but not osteoblastic MC3T3-E1 cell culture. Biomaterials 2001;22:2465–73.
[19] Aubin JE. Bone stem cells. J Cell Biochem Suppl 1998;30(/31):73–82.
[20] Steele JG, McFarland C, Dalton BA, Johnson G, Evans MD, Howlett CR, et al. Attachment of human bone cells to tissue culture polystyrene and to unmodified polystyrene: the effect of surface chemistry upon initial cell attachment. J Biomater Sci Polym Ed 1993;5:245–57.
[21] Howlett CR, Evans MD, Walsh WR, Johnson G, Steele JG. Mechanism of initial attachment of cells derived from human bone to commonly used prosthetic materials during cell culture. Biomaterials 1994;15:213–22.
[22] Kilpadi KL, Chang PL, Bellis SL. Hydroxyapatite binds more serum proteins, purified integrins, and osteoblast precursor cells than titanium or steel. J Biomed Mater Res 2001;57:258–67.
[23] Wang L, Zhao G, Olivares-Navarrete R, Bell BF, Wieland M, Cochran DL, et al. Integrin β1 silencing in osteoblasts alters substrate-dependent responses to 1,25-dihydroxy vitamin D3. Biomaterials 2006;27:3716–25.
[24] Keselowsky BG, Wang L, Schwartz Z, Garcia AJ, Boyan BD. Integrin α5 controls osteoblastic proliferation and differentiation responses to titanium substrates presenting different roughness characteristics in a roughness independent manner. J Biomed Mater Res 2007;80A:700–10.
[25] Siebers MC, ter Brugge PJ, Walboomers XF, Jansen JA. Integrins as linker proteins between osteoblasts and bone replacing materials. A critical review. Biomaterials 2005;26(2):137–46.
[26] Larson BL, Ylöstalo J, Prockop DJ. Human multipotent stromal cells undergo sharp transition from division to development in culture. Stem Cells 2008;26(1):193–201.
[27] Lincks J, Boyan BD, Blanchard CR, Lohmann CH, Liu Y, Cochran DL, et al. Response of MG63 osteoblast-like cells to titanium and titanium alloy is dependent on surface roughness and composition. Biomaterials 1998;19(23):2219–32.
[28] Boyan BD, Batzer R, Kieswetter K, Liu Y, Cochran DL, Szmuckler-Moncler S, et al. Titanium surface roughness alters responsiveness of MG63 osteoblast-like cells to 1 alpha, 25-(OH)2D3. J Biomed Mater Res 1998;39(1):77–85.
[29] Boyan BD, Lohmann CH, Sisk M, Liu Y, Sylvia VL, Cochran DL, et al. Both cyclooxygenase-1 and cyclooxygenase-2 mediate osteoblast response to titanium surface roughness. J Biomed Mater Res 2001;55(3):350–9.
[30] Lohmann CH, Tandy EM, Sylvia VL, Hell-Vocke AK, Cochran DL, Dean DD, et al. Response of normal female human osteoblasts (NHOst) to 17 beta-estradiol is modulated by implant surface morphology. J Biomed Mater Res 2002;62(2):204–13.
[31] Schneider GB, Perinpanayagam H, Clegg M, Zaharias R, Seabold D, Keller J, et al. Implant surface roughness affects osteoblast gene expression. J Dent Res 2003;82(5):372–6.
[32] Schneider GB, Zaharias R, Seabold D, Keller J, Stanford C. Differentiation of preosteoblasts is affected by implant surface microteopographies. J Biomed Mater Res A 2004;69(3):462–8.
[33] Hamilton DW, Wong KS, Brunette DM. Microfabricated discontinuous-edge surface topographies influence osteoblast adhesion, migration, cytoskeletal organization, and proliferation and enhance matrix and mineral deposition in vitro. Calcif Tissue Int 2006;78(5):314–25.
[34] Zhao G, Zinger O, Schwartz Z, Wieland M, Landolt D, Boyan BD. Osteoblast-like cells are sensitive to submicron-scale surface structure. Clin Oral Implants Res 2006;17(3):258–64.
[35] Hamilton DW, Brunette DM. The effect of substratum topography on osteoblast adhesion mediated signal transduction and phosphorylation. Biomaterials 2007;28(10):1806–19.
[36] Hamilton DW, Chehroudi B, Brunette DM. Comparative response of epithelial cells and osteoblasts to microfabricated tapered pit topographies in vitro and in vivo. Biomaterials 2007;28(14):2281–93.
[37] Dalby MJ, Gadegaard N, Tare R, Andar A, Riehle MO, Herzyk P, et al. The control of human mesenchymal cell differentiation using nanoscale symmetry and disorder. Nat Mater 2007;6:997–1003.
[38] Dalby MJ, McCloy D, Robertson M, Wilkinson C, Oreffo R. Osteoprogenitor response to defined topographies with nanoscale depths. Biomaterials 2006;27:1306–15.